COVER SHEET

A Raman spectroscopic study of the uranyl phosphate mineral parsonsite

Ray L. Frost[•], Jiří Čejka[+)], Matt Weier and Wayde N. Martens

Inorganic Materials Research Program, School of Physical and Chemical Sciences, Queensland University of Technology, GPO Box 2434, Brisbane Queensland 4001, Australia.

[+)] National Museum, Václavské náměstí 68, CZ-115 79 Praha 1, Czech Republic.

Abstract

The mineral parsonsite with samples from The Ranger Uranium Mine, Australia and La Faye Mine, Grury, Saone-et-Loire, Burgundy, France has been characterised by Raman spectrocopy at 298 and 77 K and complemented with infrared spectroscopy. Two Raman bands close to 807 and 796 cm^{-1} are attributed to the ν_1 $(UO_2)^{2+}$ symmetric stretching modes, whilst two bands close to 953 or 945 cm^{-1} and 863-873 cm^{-1} are assigned to the ν_3 $(UO_2)^{2+}$ antisymmetric stretching vibrations. Four or five bands (953, 926, 910, 883 cm^{-1}) are observed in the infrared spectrum in this region . Bands at 965-967 and 972 cm^{-1} are assigned to the ν_1 $(PO_4)^{3-}$ symmetric stretching modes and bands that are observed in the 987 to 1078 cm^{-1} to the ν_3 $(PO_4)^{3-}$ antisymmetric stretching modes. Bands at 465, 439, 406, 394 cm^{-1} (298 K) and 466, 442, 405, 395 cm^{-1} (77 K) are assigned to the split doubly degenerate ν_2 $(PO_4)^{-3}$ bending vibrations. Bands of very low intensity at 609, 595, 591, 582, 560 and 540 cm^{-1} are attributed to the split triply degenerate ν_4 $(PO_4)^{-3}$ bending modes. Bands observed at wavenumbers lower than 300 cm^{-1} are connected with the split ν_2 (δ) $(UO_2)^{2+}$ bending, ν (U-O_{ligand}), δ (U-O_{ligand}), and lattice vibrations. U-O bond lengths in uranyl are calculated frm the Raman and infrared spectra which are in agreement with those from available X-ray single crystal structure analysis of parsonsite. Short comment is given to the water content and possibility of a hydrogen bonding network in parsonsite crystal structure.

Key words: parsonite, threadgoldite, phosphate, Raman spectroscopy, U-O bond length, uranyl, molecular water

Introduction

Uranyl minerals exhibit considerable structural and chemical diversity, and reflect geochemical conditions dominant during their formation. Their crystal chemistry is necessary to be known especially for better understanding the low-temperature mineralogy and also from the environmental and hydration-oxidation alteration of spent nuclear fuel points of view [1,2]. According to Locock, [3,4] four major structural classes of inorganic uranyl phosphates and arsenates have been recognized with regards to the concept of uranyl anion sheet topology [for details see [5-7]] (a) structures containing the autunite-type sheet (autunite and metaautunite groups), (b) structures containing the phosphuranylite-type sheet (phosphuranylite group), (c) structures containing the uranophane sheet anion topology, (d) chain structures. Chain structures are relatively uncommon in natural uranyl phosphates and uranyl

[•] Author to whom correspondence should be addressed (r.frost@qut.edu.au)

arsenates and occur only in walpurgite, orthowalpurgite, hallimondite and parsonite [3,4]. The mineral parsonite is well known and widely spread worldwide (see http://www.mindat.org/show.php?id=3126).

Studies of the phosphate minerals have been undertaken for some considerable time [8-13]. The mineral parsonite of formula $Pb_2(UO_2)(PO_4)_2.nH_2O$ ($0 \le n \le 2$ or $0 \le n \le 0.5$) is one of many uranyl phosphates [14-16]. The mineral is triclinic with a = 6.842(4), b = 10.383(6), c = 6.670(4) Å, and α=101.26(7)°, β=98.17(7)°, γ=86.38(7)°, space group P(-1), Z=2 [8,17], its synthetic analogue a = 8432(5), b = 10.4105(7), c = 6.6718(4) Å, $\alpha = 101.418(1)^o$, $\beta = 98.347(2)^o$, $\gamma = 86.264(2)^o$, space group P(-1), Z = 2 [3,4]. Some attempts to study in detail the crystallography and crystal structure of parsonite were also made by Mazzi et al. [18]. Burns states that 'The single unique U^{6+} cation is present as a $(UO_2)^{2+}$ uranyl ion and is coordinated by five additional atoms of oxygen arranged at the equatorial corners of a pentagonal bipyramid capped by the O atoms of uranyl. Uranyl polyhedra share an edge-forming dimers, which are cross-linked by edge- and vertex-sharing with two distinct phosphate tetrahedra, resulting in a new uranyl phosphate chain. Two symmetrically distinct Pb^{2+} cations are coordinated by nine and six oxygen atoms, and link adjacent uranyl phosphate chains [17].' Parsonite is the first uranyl phosphate mineral structure that is based upon chains of polymerised polyhedra of higher bond-valence [17]. The structure of parsonite is shown in Figures 1a, 1b and 1c [3].The structure clearly shows two distinct Pb atoms in the structure. The phosphate in the structure is of a reduced C_{3v} symmetry. There has been a discussion about the water content in parsonite. Schoep [14,19,20] assumed the presence of one water molecule per formula unit (pfu), while Frondel [21,22] of one or two water molecules pfu, and Branche et al. [23-25] one H_2O. Bignand [26] studied natural and synthetic parsonite and inferred this phase should be anhydrous. This is supported also by Ross [15] who prepared anhydrous parsonite. According to Vochten et al. [27], synthetic parsonite contains 0.5 H_2O pfu. Burns [28] states on the X-ray single crystal structure study of parsonite this mineral is anhydrous. Locock et al. studied X-ray single crystal structure of synthetic parsonite and proposed for this compound the formula $Pb_2[(UO_2)(PO_4)_2].n\ H_2O$, where $0 \le n \le 0.5$ [3,4].Anthony et al. describe in their Handbook of Mineralogy [29] parsonite as dihydrate, whilst Mandarino and Back [30] in the famous Fleischer's Glossary of Mineral Species as anhydrous.

Infrared spectroscopy and thermal analysis of the uranyl minerals inclusive of uranyl phosphate minerals was reviewed by Čejka [31]. Neither infrared nor Raman spectra of parsonite are available. Only wavenumbers of the ν_1 and ν_3 $(UO_2)^{2+}$ stretching vibrations, force constant and calculated U-O bond lengths in uranyl inferred from the infrared spectrum of parsonite were given without any other details [32]. Luminescent spectra of parsonite are available [for details and references see Gorobets and Rogojine 2002 [33]]. Some Raman studies of uranyl phosphates have been undertaken [34-38]. The amount of published data on the Raman spectra of mineral phosphates is limited [39-43]. The Raman spectra of the hydrated or hydroxy phosphate minerals is severly limited. In aqueous systems, Raman spectra of phosphate oxyanions show a symmetric stretching mode (ν_1) at 938 cm^{-1}, the antisymmetric stretching mode (ν_3) at 1017 cm^{-1}, the symmetric bending mode (ν_2) at 420 cm^{-1} and the ν_4 mode at 567 cm^{-1} [41,42,44]. S.D. Ross in Farmer (1974) (page 404) listed some well-known minerals containing phosphate which were either hydrated or hydroxylated or both [45]. The value for the ν_1 symmetric stretching vibration of PO_4

units as determined by infrared spectroscopy was given as 930 cm^{-1} (augelite), 940 cm^{-1} (wavellite), 970 cm^{-1} (rockbridgeite), 995 cm^{-1} (dufrenite) and 965 cm^{-1} (beraunite). The position of the symmetric stretching vibration is mineral dependent and a function of the cation and crystal structure. The fact that the symmetric stretching mode is observed in the infrared spectra affirms a reduction in symmetry of the $(PO_4)^{2-}$ units.

The paper forms part of the Raman and infrared spectroscopy study of secondary minerals including uranyl minerals. Raman spectroscopy has proven most useful for the study of these uranyl bearing minerals. Whilst infrared spectroscopy provides useful information on the study of minerals containing the uranyl unit, the spectra suffer from band overlap making the attribution of the bands difficult. Raman spectroscopy on the other hand provides spectra with spectral regions in which definitive assignments of the bands can be given. In this work we report the Raman spectra of the mineral parsonsite, a mineral which has been not studied in terms of vibrational spectroscopy, and we relate the spectra to the structure of the mineral.

Experimental

Minerals

Two parsonsite mineral samples were obtained from Museum Victoria labeled m36228 and m33831. The minerals originated from the Ranger Uranium Mine and the La Faye Mine, Grury, Saone-et-Loire, Burgundy, France. A second sample from La Faye Mine, Grury, Saone-et-Loire, Burgundy, France was obtained from the Mineralogic Research Company.

The analysis of the mineral parsonsite (sample m33831) from La Faye Mine, Grury, Saone-et-Loire, Burgundy, France, gave UO_3 32.1 %, P_2O_5 16.25%, PbO 48.53%. This data leads to a formula of $Pb_2[(UO_2)(PO_4)_2].2\ H_2O$. Thermal analysis gave a mass loss of 4.52% which is slightly high for 2 moles of water per formula unit. A mineral sample of parsonsite from Ruggles Mine, New Hampshire, USA gave chemical analyses of UO_3 33.6 %, P_2O_5 15.05%, PbO 48.23% [46]. This data leads to a formula of $Pb_2[(UO_2)(PO_4)_2].2\ H_2O$. A parsonsite mineral sample from Kasolo, Shaba, Democratic Republic of Congo gave analyses of UO_3 29.66 %, P_2O_5 15.59%, PbO 49.03% and H_2O as 3.96 %. This also leads to a formula $Pb_2[(UO_2)(PO_4)_2].2\ H_2O$.

Raman microprobe spectroscopy

The crystals of parsonite were placed and orientated on the stage of an Olympus BHSM microscope, equipped with 10x and 50x objectives and part of a Renishaw 1000 Raman microscope system, which also includes a monochromator, a filter system and a Charge Coupled Device (CCD). Raman spectra were excited by a HeNe laser (633 nm) at a resolution of 2 cm^{-1} in the range between 100 and 4000 cm^{-1}. Repeated acquisition using the highest magnification was accumulated to improve the signal to noise ratio. Spectra were calibrated using the 520.5 cm^{-1} line of a silicon wafer. In order to ensure that the correct spectra are obtained, the incident excitation radiation was scrambled. Previous studies by the authors provide more details of the experimental technique [47-58]. The Raman spectra of the oriented single

crystals are reported in accordance with the Porto notation.

It should be noted that because of the very small amount of sample supplied on loan from the museum, it was not possible to run the infrared spectra od some of the samples. This does show a major advantage of Raman spectroscopy in the study of uranium minerals is the ability to study very small amounts of mineral. Spectra at liquid nitrogen temperature were obtained using a Linkam thermal stage (Scientific Instruments Ltd, Waterfield, Surrey, England). Details of the technique have been published elsewhere by the authors [47,48,59-63]

Infrared spectroscopy

Infrared spectra were obtained using a Nicolet Nexus 870 FTIR spectrometer with a smart endurance single bounce diamond ATR cell. Spectra over the 4000–525 cm^{-1} range were obtained by the co-addition of 64 scans with a resolution of 4 cm^{-1} and a mirror velocity of 0.6329 cm/s.Spectra were co-added to improve the signal to noise ratio.

In this experiment it should be noted that Raman spectra were obtained using a Renishaw Raman microscope and these spectra are compared with the infrared spectra obtained by using a single bounce diamond ATR cell. The Raman spectra are obtained from a sample size of 1 micron whereas the infrared spectra are collected from a sample size of at best 25 microns. The Raman spectra are thus obtained from a significantly smaller sample size. In the normal course of events Raman spectra are obtained from a number of crystals and from different positions on the same crystal. This ensures that typical mineral spectra are obtained. It should be noted that a comparison is being made between a microRaman spectrum which is orientation dependent with an infrared spectrum which is essentially from a bulk sample.

Spectroscopic manipulation such as baseline adjustment, smoothing and normalisation were performed using the Spectracalc software package GRAMS (Galactic Industries Corporation, NH, USA). Band component analysis was undertaken using the Jandel 'Peakfit' software package, which enabled the type of fitting, function to be selected and allows specific parameters to be fixed or varied accordingly. Band fitting was done using a Gauss-Lorentz cross-product function with the minimum number of component bands used for the fitting process. The Gauss-Lorentz ratio was maintained at values greater than 0.7 and fitting was undertaken until reproducible results were obtained with squared correlations of r^2 greater than 0.995.

Results and discussion

In the crystal structure of parsonsite, there is only symmetrically distinct U^{6+} in the form of uranyl units, and two symmetrically distinct P^{5+} as $(PO_4)^{3-}$ units with two molecules in the unit cell [3,4]. The symmetry of free uranyl and phosphate units is therefore lowered. Raman and infrared activation of all vibrations and splitting of the doubly [the ν_2 $(UO_2)^{2+}$ bending vibration and the ν_2 $(PO_4)^{3-}$ bending vibration] and triply [the ν_3 antisymmetric stretching vibration and the ν_4 $(PO_4)^{3-}$bending vibration]

degenerate vibrations is therefore expected depending on site symmetry of individual units.

Raman spectroscopy

Uranyl, $(UO_2)^{2+}$, and Phosphate, $(PO_4)^{3-}$, stretching vibrations

The Raman spectra of three samples of parsonsite at 298 and 77 K together with the room temperature infrared spectra in the 500 to 1200 cm^{-1} region are shown in Figure 2a and 2b. The results of the Raman spectral analysis is reported in Table 1. The infrared spectrum clearly shows a broad band profile in contrast to the sharp well resolved bands in the Raman spectra. Two sets of bands are observed centred upon 810 and 960 to 1030 cm^{-1}. The band centred upon 810 cm^{-1} is asymmetric on the low wavenumber side and two bands may be resolved at 807 and 796 cm^{-1} (Ranger U mine sample). These bands are assigned to the ν_1 symmetric stretching mode of the $(UO_2)^{2+}$ units. The low intensity band at 790 cm^{-1} in the infrared spectrum is the infrared equivalent of the symmetric stretching vibrations of the $(UO_2)^{2+}$ units (Figure 2 ATR spectrum). For the Ranger uranium mine sample hese bands shift to 810 and 804 cm^{-1} upon obtaining the spectra at 77 K. These bands are not observed in the infrared spectra which consists of a broad profile of overlapping bands. A low intensity band at 800 cm^{-1} is the infrared forbidden $(UO_2)^{2+}$ symmetric stretching mode. An intense band at 845 cm^{-1} in the infrared spectrum is assigned to a water librational mode. Low intensity bands are observed around 872 cm^{-1} which may be attributed to this vibration.

The wavenumber region of expected bands which may be attributed to the ν_1 $(UO_2)^{2+}$ symmetric stretching vibrations was calculated with the empirical relations $\nu_1 = 0.94\nu_3(UO_2)^{2+}$ cm^{-1}, $\nu_1 = 0.89\nu_3(UO_2)^{2+} + 21$ cm^{-1} [for details see e.g. Čejka [31]] and $\nu_1 = 0.795\nu_3(UO_2)^{2+} + 107$ cm^{-1} [64]. An intense band at 845 cm^{-1} in the infrared spectrum and low intensity bands observed in the Raman around 872 cm^{-1} may be attributed to the ν_3 $(UO_2)^{2+}$ antisymmetric stretching vibrations. In the case of the band at 845 cm^{-1}, there may be a confusion with the ν_1 $(UO_2)^{2+}$. An empirical relation $R_{U-O} = 106.5\nu_1(UO_2)^{2+} + 0.575$ Å [65] was used for the calculation of the U-O bond lengths with the following results (Å/cm^{-1}; 298 K//77 K) Raman : Ranger U mine sample - 1.780/831, 1.804/807, 1.815/796// 1.801/810, 1.807/804; La Faye Mine sample 1 - 1.804/807, 1.822/789// 1.771/840, 1.802/809, 1.814/797; La Faye Mine sample 2 - 1.804/807, 1.815/796, 1.803/808, 1.816/795; IR: La Faye Mine sample 2 - 1.767/845, 1.811/800, 1.821/790. The U-O bond lengths in uranyl inferred from the X-ray single crystal structure of natural parsonsite are 1.75(2) and 1.82(2), on average 1.785 Å [66] and for synthetic parsonsite 1.770(6) and 1.784(6), on average 1.777 Å [3,4] are in good agreement with the values calculated from the wavenumber of the ν_1 $(UO_2)^{2+}$ and those proposed for natural and synthetic uranyl phases [5-7].

Bands observed in the range from 845 to 954 cm^{-1} are attributed to the ν_3 $(UO_2)^{2+}$ antisymmetric stretching vibrations. In the infrared spectrum a band at 953 cm^{-1} is attributed to this vibration. An empirical relation $R_{U-O} = 91.41\nu_3(UO_2)^{-2/3} + 0.804$ Å [65] enables to calculate the U-O bond lengths (Å) in uranyl form the infrared and/or Raman spectra. The results are as follows (Å/cm^{-1};298 K//77 K) Raman: Ranger U Mine sample 1.755/943, 1.805/872//1.753/946, 1.805/873; La Faye Mine sample 1 1.812/864// 1.753/945, 1.807/870; La Faye Mine sample 2 1.747/954,

1.810/866// 1.753/945, 1.809/868; IR 1.748/953, 1.766/926' 1.777/910, 1.797/883 and 1.827/845. All these values are also close to those from the X-ray single crystal structure analysis of parsonsite.

The phosphate bands are of very low intensity (Figure 2b). Some recent studies have shown that the intensity of phosphate bands may be of a very low intensity in autunites minerals because of low symmetry [35,67]. However, some confusion with the ν_1 $(PO_4)^{3-}$ vibrations is possible, especially in the case of the bands at 953 and 952 cm^{-1}, respectively. These bands are assigned to the ν_3 $(UO_2)^{2+}$ vibrations rather than the ν_1 $(PO_4)^{3-}$ vibrations. The intensity of the ν_3 $(UO_2)^{2+}$ antisymmetric stretching bands would be expected to be of a low intensity. In the infrared spectrum a broad intense band at 953 cm^{-1} is ascribed to this band. The bands at 967 (298 K), 972 (77 K) for the Ranger sample and 968 cm^{-1} (298 and 77 K) are assigned to the ν_1 $(PO_4)^{3-}$ symmetric stretching modes. For the La Faye mine sample 1 it is noted that two bands are observed at 972 and 965 cm^{-1} in both the 298 and 77 K spectra. This suggests there are two independent phosphates in the unit cell. An alternative analysis based upon the alternativity of the Raman bands (1078, 1024 and 988 cm^{-1}) and the infrared bands (1097, 1030 and 995 cm^{-1}) of the triply degenerate phosphate antisymmetric stretching modes supports the concept of lattice splittings due to weak vibrational coupling between the phosphate units. No bands are observed in this position in the infrared spectra. These observations assist with the assignment of bands at around 953 cm^{-1} to the ν_3 $(UO_2)^{2+}$ antisymmetric stretching vibration and the bands at 965-967 and 972 cm^{-1} to the ν_1 $(PO_4)^{3-}$ symmetric stretching modes. The bands that are observed in the 987 to 1078 cm^{-1} region are assigned to the ν_3 $(PO_4)^{3-}$ antisymmetric stretching modes. The bands are of relatively low intensity in the Raman spectra. Three intense bands are observed in the infrared spectra at 1097, 1030 and 995 cm^{-1} which may be assigned to these vibrations. For the Ranger mine sample, Raman bands are observed at 1078, 1024, 998 and 987 cm-1 (298 K) and at 1080, 1026, 988 cm^{-1} (77K). Bands are observed in similar positions for the La Faye mine sample 2.

Phosphate, $(PO_4)^{3-}$, bending vibrations

The Raman spectra of the low wavenumber region are shown in Figure 3. It is clear that the spectra may be subdivided into two spectral regions namely 350 to 500 cm^{-1} and 100 to 300 cm^{-1}. The first region defines the phosphate bending modes and the second region the OUO bending and PbO stretching and bending vibrations. Wavenumbers of the bands of the $(PO_4)^{3-}$ bending vibrations are located in the region 391-615 cm^{-1}. Bands at (465,439, 406, 394 cm^{-1}) (298 K), and (399, 416, 449 and 490 cm^{-1}) and (466, 442, 405, 395 cm^{-1}) (77 K) are assigned to the split doubly degenerate ν_2 $(PO_4)^{3-}$ bending vibrations. Some slight variation in the band position occurs between the samples. Also there is an apparent slight shift to lower wavenumbers upon cooling to 77 K. Infrared bands in this spectral region were not obtained, as the lower wavenumber cutoff of the ATR diamond cell is 550 cm^{-1}.

Bands in the infrared spectrum between 550 and 650 cm^{-1} were obtained. This spectral region is the region of the ν_4 bending modes. In the infrared spectrum two broadish bands at 607 and 568 cm^{-1} are observed (Figure 4). Multiple bands are observed in the Raman spectrum in this spectral region. The bands are of very low intensity and limited by the signal to noise ratio. For the ranger uranium mine sample

bands are found at 609, 595, 591, 582, 560 and 540 cm^{-1}. The bands show a shift to higher wavenmumbers upon cooling to 77 K. The bands are observed at 610, 597, 584, 563 and 540 cm^{-1}. These bands are attributed to the split triply degenerate ν_4 $(PO_4)^{3-}$ bending vibrations.

Uranyl, $(UO_2)^{2+}$, bending vibrations

The spectral patterns in the 100 to 300 cm^{-1} are similar for the three samples analysed and at the two temperatures. Bands observed at lower wavenumbers than 300 cm^{-1} are assigned to the ν_2 (δ) $(UO_2)^{2+}$ and ν (U-O_{ligand}) and δ(U-O_{ligand}) vibrations without any detailed attribution. Three bands are observed at 281, 255 and 206 cm^{-1}. The bands are observed at 280, 258 and 209 cm^{-1} at 77 K. The intense band at ~151 cm^{-1} is ascribed to PbO symmetric stretching vibrations.

Water stretching vibrations

The available formulae for parsonite indicate that this mineral may be anhydrous or contain up two moles of water per formula unit, as discussed in the introduction. However, quality of the recorded Raman spectra in the region of the OH stretching vibrations is not good (Figure 5). Water is inherently very difficult to measure using Raman spectroscopy as water is a very poor scatterer of the incident radiation. Any interpretation makes therefore problems. On the other side, the recorded infrared spectrum of parsonite seems to be very complicated in this region which does not correspond with any small amount of water contained in the crystal structure of parsonite of $Pb_2[(UO_2)(PO_4)_2].2\ H_2O$. The two moles of water would give significant intensity in the infrared spectrum.

The formula for parsonite indicates the presence of two moles of water. The water stretching vibrations are shown in Figure 5. The infrared spectrum indicates at least three broad bands at 3564, 3451 and 3262 cm^{-1}. These bands may be assigned to water OH stretching vibrations. Additional bands at 3699, 3678, 3632 and 3623 cm^{-1} may be due to an impurity or alternatively may be probably assigned to MOH stretching bands. In the Raman spectrum of the Ranger sample two bands are observed at 3404 cm^{-1} (very broad) and at 3329 cm^{-1} (sharp). For the La Faye mine sample 1 only the band at 3331 cm^{-1} is observed. The Raman spectrum of the La Faye mine sample 2 shows a pattern similar to that of the Ranger sample. Two bands are observed at 3384 and 3327 cm^{-1}. In the infrared spectrum of parsonite an intense band is observed at 1639 cm^{-1}. The band is attributed to the water bending mode. The position of the band is indicative of strong hydrogen bonding between the water molecules and the phosphate units.

In the infrared spectrum of parsonite an intense band is observed as 1639 cm^{-1}, which may be related to the Raman bands at 1590 cm^{-1} (Ranger U Mine sample, 298 K) and 1602 cm^{-1} (La Faye Mine 2 sample, 77 K). These bands are attributed to the δ H_2O bending mode. Any comments to the hydrogen bonding network which may be expected do not seem possible to be unambiguously made. As may be seen in the Table 1, some bands in the region of vibrations of uranyl and phosphate units may be probably connected with libration modes of water molecules,

however, this is very questionable because of an unclear role of not well defined amount of water in the crystal structure of parsonsite. According to Locock [3,4], this molecular water may not be important for the origin and stability of parsonsite under natural conditions. However, according to these authors, analysis of cavities in the structure of parsonsite reveals that the position centered as 0, 0, 1/2 is the only significant void in the structure and the only candidate for the presence of structural water. Locock [3,4] understand this cavity large enough to contain water. This is supported by their FTIR spectrum of synthetic parsonsite, presented without any interpretation, and thermogravimetric analysis of synthetic parsonsite by Vochten et al. [68].Locock therefore suggests that the water content in parsonsite could be variable and proposes the formula $Pb_2[(UO_2)(PO_4)_2](H_2O]_n$. This formula is analogous to that of hallimondite, $Pb_2[(UO_2)(PO_4)_2](H_2O)_n$, in which $0 \leq n \leq 0.5$. The only conclusion that may be made from the Raman and infrared spectra of parsonsite samples studied is that they may contain molecular water without any detailed resolution, and that some most probably very weak hydrogen bonds may be present in the parsonsite crystal structure. Broad band observed especially at 3262 cm^{-1} in the infrared spectrum of the La Faye Mine 2 sample (Table 1, Figure 3) may prove the presence of a strong hydrogen bonding network, however, this band may be connected with some impurities the presence of which in this sample is supposed.

Conclusions

Raman spectra of two samples of parsonsite measured at 298 and 77 K, and infrared spectrum of one of these samples are presented and interpreted with regard to the $(UO_2)^{2+}$ and $(PO_4)^{3-}$ stretching and bending vibrations. Short comment is given to the role of water in the crystal structure of parsonsite. U-O bond lengths in uranyls are calculated with available empirical relations $R_{U-O} = f[\nu_1(UO_2)^{2+}]$ and $R_{U-O} = f[\nu_3(UO_2)^{2+}]$ and compared with those from published X-ray single crystal structure data of parsonsite.

Acknowledgements

The financial and infra-structure support of the Queensland University of Technology Inorganic Materials Research Program of the School of Physical and Chemical Sciences is gratefully acknowledged. The Australian Research Council (ARC) is thanked for funding the instrumentation used in this work.

References

1. Burns, PC. *Mat. Res. Soc. Symp. Proc.* 2004**; 802**: DD3.2.1.
2. Burns, PC. *Proceedings of the Russian Mineralogical Society* 2003**; 132**: 90.
3. Locock, AJ, Burns, PC, Flynn, TM. *American Mineralogist* 2005**; 90**: 240.
4. Locock, AJ. *PhD*, Notre Dame 2004.
5. Burns, PC, Miller, ML, Ewing, RC. *Canadian Mineralogist* 1996**; 34**: 845.
6. Burns, PC, Ewing, RC, Hawthorne, FC. *Canadian Mineralogist* 1997**; 35**: 1551.
7. Burns, PC. *Reviews in Mineralogy* 1999**; 38**: 23.
8. Suzuki, Y, Murakami, T, Kogure, T, Isobe, H, Sato, T. *Materials Research Society Symposium Proceedings* 1998**; 506**: 839.
9. Chernorukov, NG, Suleimanov, EV, Ermonin, SA. *Russian Journal of General Chemistry (Translation of Zhurnal Obshchei Khimii)* 2002**; 72**: 161.
10. Barinova, AV, Rastsvetaeva, RK, Sidorenko, GA, Chukanov, NV, Pushcharovskii, DY, Pasero, M, Merlino, S. *Doklady Chemistry (Translation of the chemistry section of Doklady Akademii Nauk)* 2003**; 389**: 58.
11. Locock, AJ, Burns, PC. *Canadian Mineralogist* 2003**; 41**: 91.
12. Locock, AJ, Burns, PC. *Journal of Solid State Chemistry* 2002**; 167**: 226.
13. Majumdar, D, Balasubramanian, K. *Chemical Physics Letters* 2004**; 397**: 26.
14. Schoep, A. *Comptes Rendus de l'Academie des Sciences, Paris* 1923**; 176**: 171.
15. Ross, V. *American Mineralogist* 1956**; 41**: 915.
16. Sevchenko, AN, Umreiko, DS. *Uchenye Zapiski, Belorus. Gosudarst. Univ. im. V. I. Lenina, Ser. Fiz.* 1958: 27.
17. Burns, PC. *American Mineralogist* 2000**; 85**: 801.
18. Mazzi, F, Garavelli, CL, Rinaldi, F. *Atti Società Toscana di Scienze naturali* 1958**; A65**: 135.
19. Schoep, A. *Annales du Musee du Congo Belge, Ser. I, Minéral., Tervuren* 1930**; 1**: 43.
20. Schoep, A. *Bulletin de la Societe Belge de Geologie, de Paleontologie et d'Hydrologie* 1923**; 33**: 169.
21. Frondel, C *Systematic Mineralogy of Uranium and Thorium*, 1958.
22. Frondel, C. *American Mineralogist* 1950**; 35**: 245.
23. Chervet, J *Les minéraux secondaires*; **Institut National des Sciences et Techniques Nucléaires Saclay- Presses Universitaires de France**: Paris, France, 1960.
24. Chervet, J, Branche, G. *Sciences de la Terre* 1955**; 3**: 1.
25. Branche, G, Chervet, J, Guillemin, C. *Bull. de la Société française de Minéralogie et Cristallographie* 1951**; 54**: 457.
26. Bignand, C. *Bulletin de la Société française de Minéralogie et Cristallographie* 1955**; 78**: 1.
27. Vochten, R, Haverbeke, LV, Springel, KV. *Neues Jahrbuch fuer Mineralogie, Monatshefte* 1991**; H 12**: 551.
28. Burns, PC, Hill, FC. *Canadian Mineralogist* 2000**; 38**: 163.
29. Anthony, JW, Bideaux, RA, Bladh, KW, Nichols, MC *Handbook of Mineralogy*; Mineral Data Publishing: Tiscon, Arizona, USA, 2003; Vol. 5.

30. Mandarino, JA, Back, ME *Fleischer's Glossary of Mineral Species*; The Mineralogical Record Inc.: Tucson, Arizona, U. S. A, 2004.
31. Cejka, J. *Reviews in Mineralogy* 1999**; 38**: 521.
32. Matkovskii, AO, Gevork'yan, SV, Povarennykh, AS, Sidorenko, GA, A. N. Tarashchan. *Mineral. Sbornik* 1979**; 33**: 11.
33. Gorobets, BS, Rogojine, AA; All-Russia Institute of Mineral Resources (VIMS): Moscow, 2002.
34. Frost, RL, Weier, M. *Spectrochimica Acta, Part A: Molecular and Biomolecular Spectroscopy* 2004**; 60**: 2399.
35. Frost, RL. *Spectrochimica Acta, Part A: Molecular and Biomolecular Spectroscopy* 2004**; 60A**: 1469.
36. Frost, RL, Erickson, KL. *Spectrochimica Acta, Part A: Molecular and Biomolecular Spectroscopy* 2004**; 61A**: 45.
37. Frost, RL, Weier, M. *Neues Jahrbuch fuer Mineralogie, Monatshefte* 2004: 575.
38. Frost, RL, Kristof, J, Weier, ML, Martens, WN, Horvath, E. *Journal of Thermal Analysis and Calorimetry* 2005**; 79**: 721.
39. Frost, RL, Duong, L, Martens, W. *Neues Jahrbuch fuer Mineralogie, Monatshefte* 2003: 223.
40. Frost, RL, Martens, W, Williams, PA, Kloprogge, JT. *Journal of Raman Spectroscopy* 2003**; 34**: 751.
41. Frost, RL, Martens, W, Williams, PA, Kloprogge, JT. *Mineralogical Magazine* 2002**; 66**: 1063.
42. Frost, RL, Williams, PA, Martens, W, Kloprogge, JT, Leverett, P. *Journal of Raman Spectroscopy* 2002**; 33**: 260.
43. Frost, RL, Williams, PA, Martens, W, Kloprogge, JT. *Journal of Raman Spectroscopy* 2002**; 33**: 752.
44. Frost, RL, Martens, WN, Kloprogge, T, Williams, PA. *Neues Jahrbuch fuer Mineralogie, Monatshefte* 2002: 481.
45. Farmer, VC *Mineralogical Society Monograph 4: The Infrared Spectra of Minerals*, 1974.
46. Anthony, JW, Bideaux, RA, Bladh, KW, Nichols, MC *Handbook of Mineralogy Vol.IV. phosphates, arsenates and vanadates*; Mineral Data Publishing: Tucson, Arizona, 2003; Vol. 4.
47. Frost, RL, Erickson, KL, Cejka, J, Reddy, BJ. *Spectrochimica Acta, Part A: Molecular and Biomolecular Spectroscopy* 2005**; 61**: 2702.
48. Frost, RL, Erickson, KL, Weier, ML, Carmody, O, Cejka, J. *Journal of Molecular Structure* 2005**; 737**: 173.
49. Frost, RL. *Journal of Raman Spectroscopy* 2004**; 35**: 153.
50. Frost, RL. *Analytica Chimica Acta* 2004**; 517**: 207.
51. Frost, RL, Duong, L, Weier, M. *Spectrochimica Acta, Part A: Molecular and Biomolecular Spectroscopy* 2004**; 60**: 1853.
52. Frost, RL, Duong, L, Weier, M. *Neues Jahrbuch fuer Mineralogie, Abhandlungen* 2004**; 180**: 245.
53. Frost, RL, Henry, DA, Erickson, K. *Journal of Raman Spectroscopy* 2004**; 35**: 255.
54. Frost, RL, Weier, M. *Neues Jahrbuch fuer Mineralogie, Monatshefte* 2004: 445.
55. Frost, RL, Weier, ML. *Journal of Raman Spectroscopy* 2004**; 35**: 299.

56. Frost, RL, Williams, PA. *Spectrochimica Acta, Part A: Molecular and Biomolecular Spectroscopy* 2004**; 60**: 2071.
57. Frost, RL, Williams, PA, Martens, W, Leverett, P, Kloprogge, JT. *American Mineralogist* 2004**; 89**: 1130.
58. Frost, RL. *Spectrochimica Acta, Part A: Molecular and Biomolecular Spectroscopy* 2003**; 59A**: 1195.
59. Frost, RL, Erickson, KL, Weier, ML, Carmody, O. *Spectrochimica Acta, Part A: Molecular and Biomolecular Spectroscopy* 2005**; 61A**: 829.
60. Frost, RL, Weier, ML, Bostrom, T, Cejka, J, Martens, W. *Neues Jahrbuch fuer Mineralogie, Abhandlungen* 2005**; 181**: 271.
61. Frost, RL, Wills, R-A, Weier, ML, Martens, W. *Journal of Raman Spectroscopy* 2005**; 36**: 435.
62. Frost, RL, Carmody, O, Erickson, KL, Weier, ML, Cejka, J. *Journal of Molecular Structure* 2004**; 703**: 47.
63. Frost, RL, Carmody, O, Erickson, KL, Weier, ML, Henry, DO, Cejka, J. *Journal of Molecular Structure* 2004**; 733**: 203.
64. Gál, M, Goggin, PL, Mink, J. *Journal of Molecular Structure* 1984**; 114**: 459.
65. Bartlett, JR, Cooney, RP. *Journal of Molecular Structure* 1989**;** 193: 295.
66. Burns, PC. American Mineralogist 2000; 85: 801.
67. Frost, RL. Neues Jahrbuch fuer Mineralogie, Monatshefte 2004: 145.
68. Vochten, R, Van Haverbeke, L, Van Springel, K. Neues Jahrbuch fuer Mineralogie, Monatshefte 1991: 551.

Ranger U Mine 298K		Ranger U Mine 77K		La Faye Mine 1 298K		La Faye Mine 1 77K		La Faye Mine 2 298K		La Faye Mine 2 77K		La Faye Mine 2 ATR		Assignment
Center (cm^{-1})	FWHM (cm^{-1})	**Center (cm^{-1})**	FWHM (cm^{-1})	**Center (cm^{-1})**	FWHM (cm^{-1})	**Center (cm^{-1})**	FWHM (cm^{-1})	**Center (cm^{-1})**	FWHM (cm^{-1})	**Center (cm^{-1})**	FWHM (cm^{-1})	**Center (cm^{-1})**	FWHM (cm^{-1})	
												3699	23	OH stretching adsorbed water
												3678	39	OH stretching adsorbed water
												3632	77	OH stretching adsorbed water
												3623	17	OH stretching adsorbed water
												3564	123	Water OH stretching
3404	280							**3384**	300			**3451**	231	„
3329	32			**3331**	51			**3327**	31			**3262**	359	„
1590	86									**1602**	24	**1639**	73	Water OH bending
												1424	66	Not known
												1377	25	„
												1355	62	„
												1170	31	$(PO_4)^{3-}$ antisymmetric stretching
1078	21	**1080**	26	**1081**	74	**1079**	23	**1077**	44	**1081**	22	**1097**	68	$(PO_4)^{3-}$ antisymmetric stretching
1074	99													„
		1047	8									**1030**	58	„

1024	31	**1026**	24	**1022**	40	**1026**	29	**1024**	33	**1025**	23			„
998	28							**1000**	23			**995**	42	„
														$(PO_4)^{3-}$ symmetric stretching
987	12	**988**	21			**988**	15	**987**	11	**989**	12			
967	19	**972**	7	**967**	9	**971**	8	**968**	15	**968**	14			„
		965	12	**963**	54	**966**	14							„
														$(UO_2)^{2+}$ antisymmetric
943	25	**946**	20			**945**	19	**954**	38	**945**	19	**953**	70	stretching
												926	25	„
												910	20	„
														$(UO_2)^{2+}$ antisymmetric stretching or water
872	38	**873**	29	**864**	32	**870**	32	**866**	45	**868**	17	**883**	47	libration
831	8					**840**	20					**845**	81	„
														$(UO_2)^{2+}$ symmetric stretching
807	12	**810**	9	**807**	22	**809**	12	**807**	13	**808**	12			
796	34	**804**	28	**789**	33	**797**	35	**796**	31	**795**	31	**800**	10	„
		778	37									**790**	35	„
												755	70	
												692	31	
										678	24	**668**	78	
														$(PO_4)^{3-}$ ν_4
609	10	**610**	8	**610**	11	**610**	11	**610**	9	**606**	32	**607**	18	bending
595	6	**597**	11	**595**	7			**595**	10					„
591	29	**584**	9	**582**	12	**587**	26	**583**	10					„
582	4													„
560	13	**563**	12					**557**	12			**568**	22	„
540	10	**540**	17			**540**	6	**540**	6			**528**	9	„
												525	114	

												$(PO_4)^{3-}$ ν_2
465	15	**466**	13	**467**	22	**467**	9	**466**	15	**466**	14	bending
439	16	**442**	13	**439**	21	**442**	13	**440**	15	**441**	19	„
406	10	**405**	8	**402**	27	**403**	11	**405**	10	**403**	19	„
394	17	**395**	20			**394**	7	**394**	13			„
						283	37	**291**	7			
												$(UO_2)^{2+}$
281	26	**280**	23	**281**	26	**281**	6	**282**	26	**282**	28	bending
255	20	**258**	17	**256**	30	**256**	20	**255**	19	**258**	12	„
227	25	**228**	23	**228**	22	**228**	25	**225**	29			„
206	25	**209**	14	**205**	27	**209**	22	**206**	21	**208**	19	„
188	20	**191**	17			**190**	17	**189**	17	**190**	12	„
171	17	**174**	8			**171**	6	**171**	16			PbO
155	20	**151**	21	**151**	25	**151**	23	**154**	22	**151**	24	„
136	23							**132**	14			„
111	11	**113**	8	**113**	15	**112**	13	**118**	15	**114**	11	Lattice
								107	8			„

Table 1 Results of theRaman spectra at 298 and 77 K of parsonsite and the infrared spectrum of parsonsite

List of Figures

List of Tables

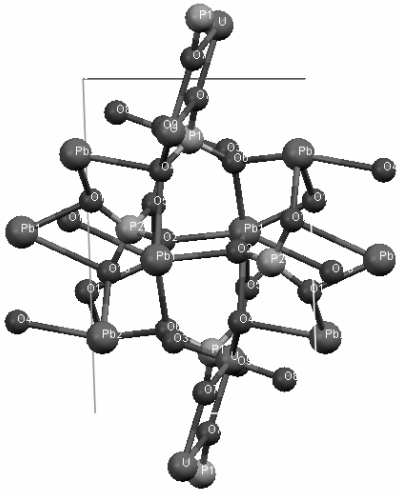

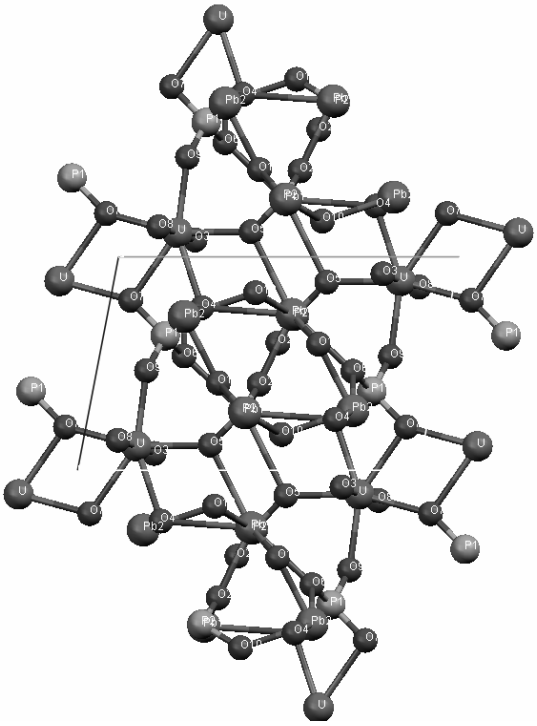

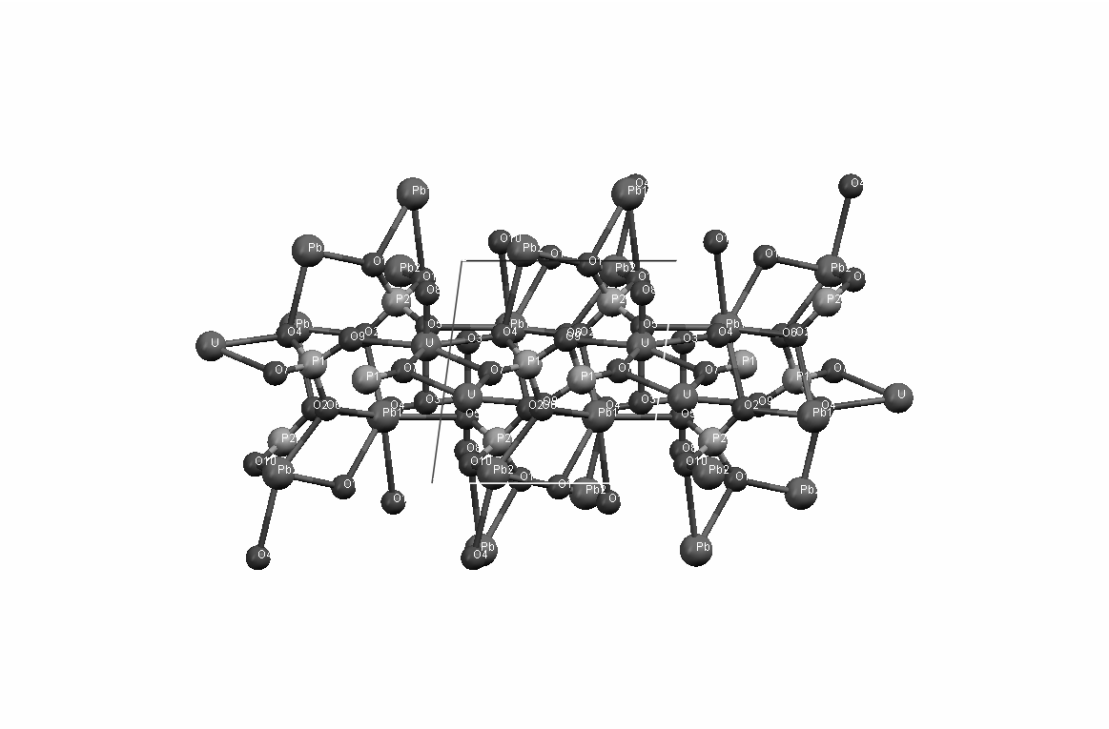

Figure 1 a,b,c

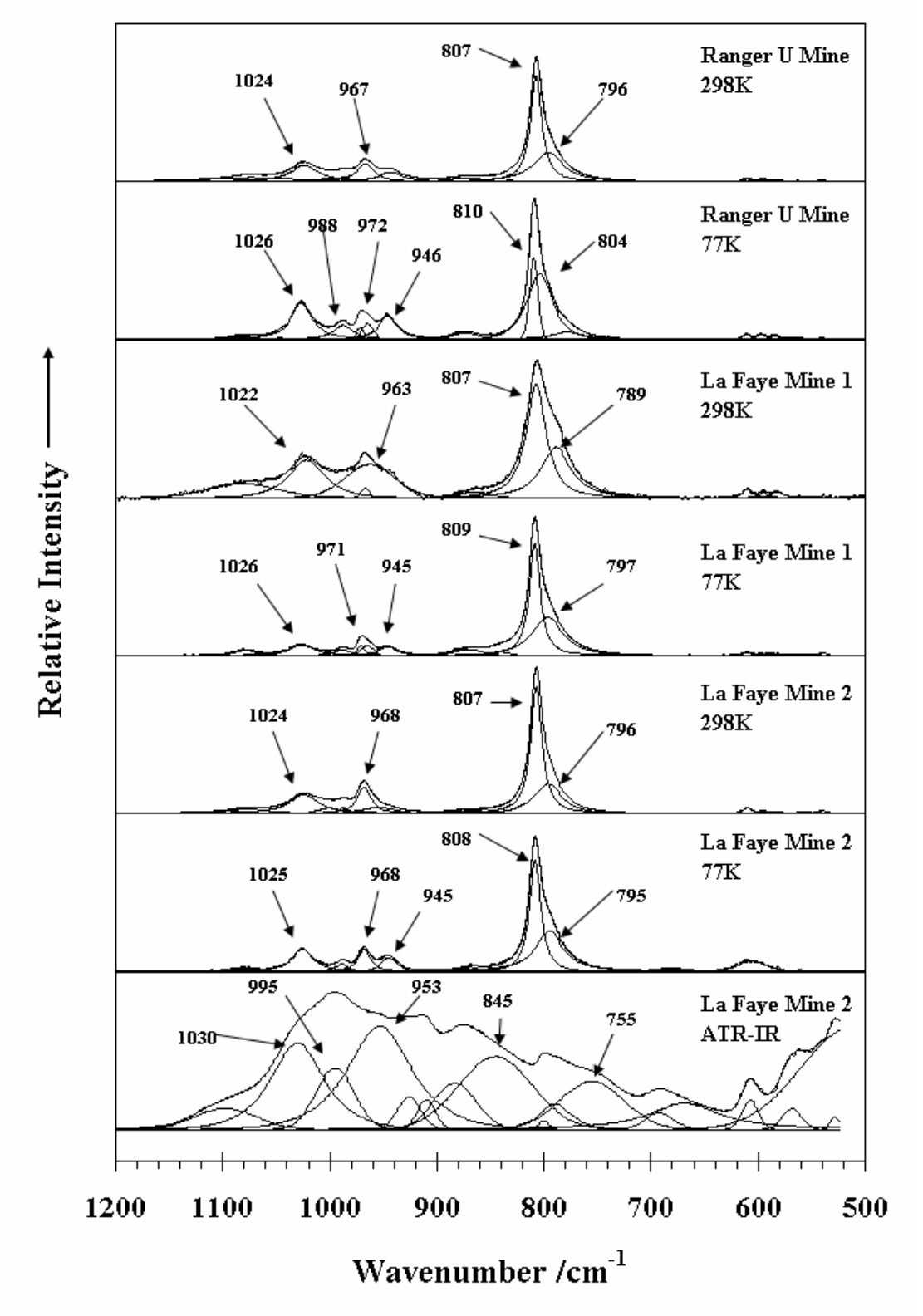
Relative Intensity
Ranger U Mine
298K
807
1024
967
796
Ranger U Mine
77K
810
988
972
1026
946
804
La Faye Mine 1
298K
807
1022
963
789
La Faye Mine 1
77K
809
971
1026
945
797
La Faye Mine 2
298K
807
1024
968
796
La Faye Mine 2
77K
808
1025
968
945
795
La Faye Mine 2
ATR-IR
995
953
845
1030
755
1200
1100
1000
900
800
700
600
500
Wavenumber /cm-1

Figure 2a

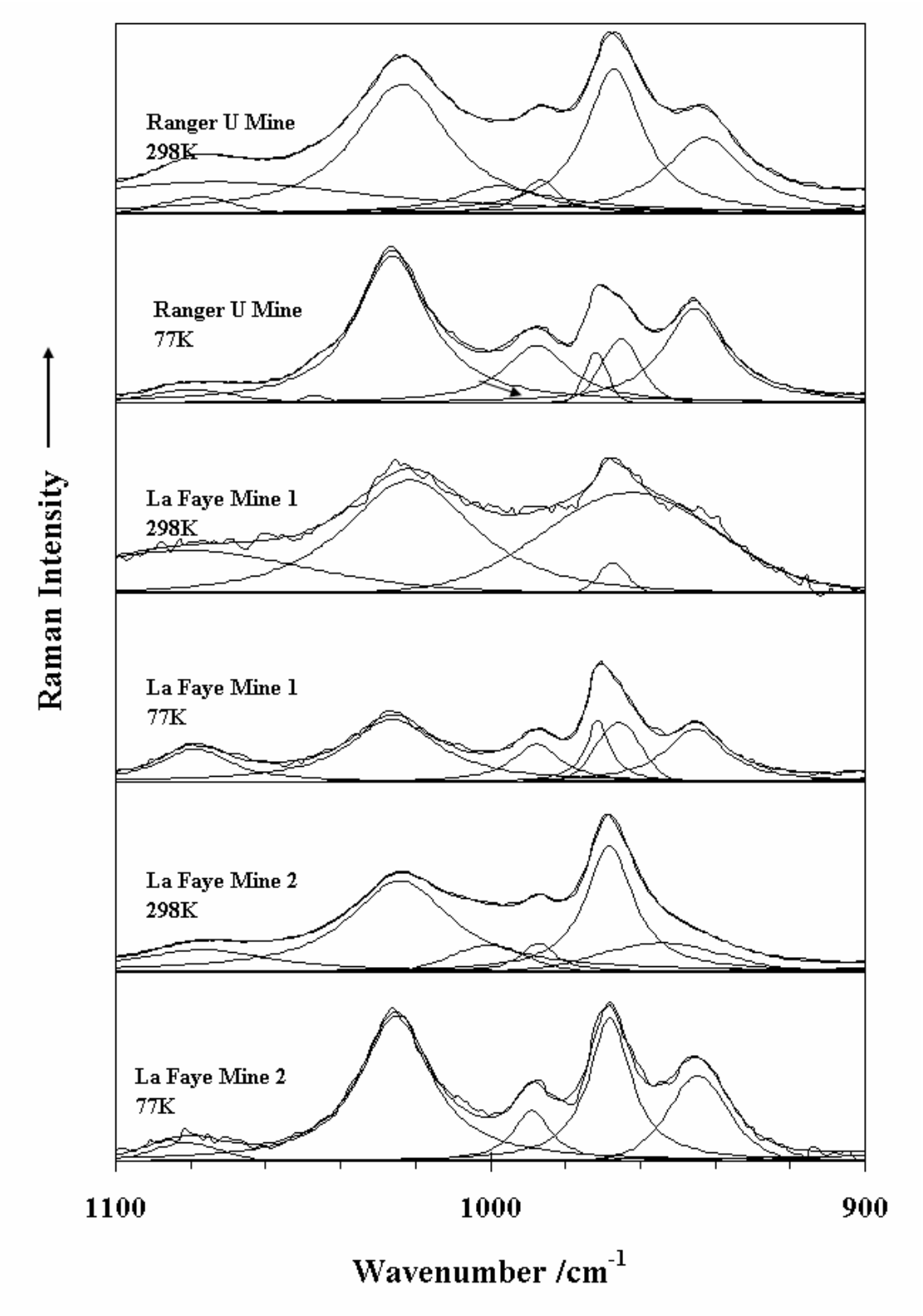
Ranger U Mine
298K
Ranger U Mine
77K
La Faye Mine 1
298K
La Faye Mine 1
77K
La Faye Mine 2
298K
La Faye Mine 2
77K
Raman Intensity
1100
1000
900
Wavenumber /cm-1

Figure 2b

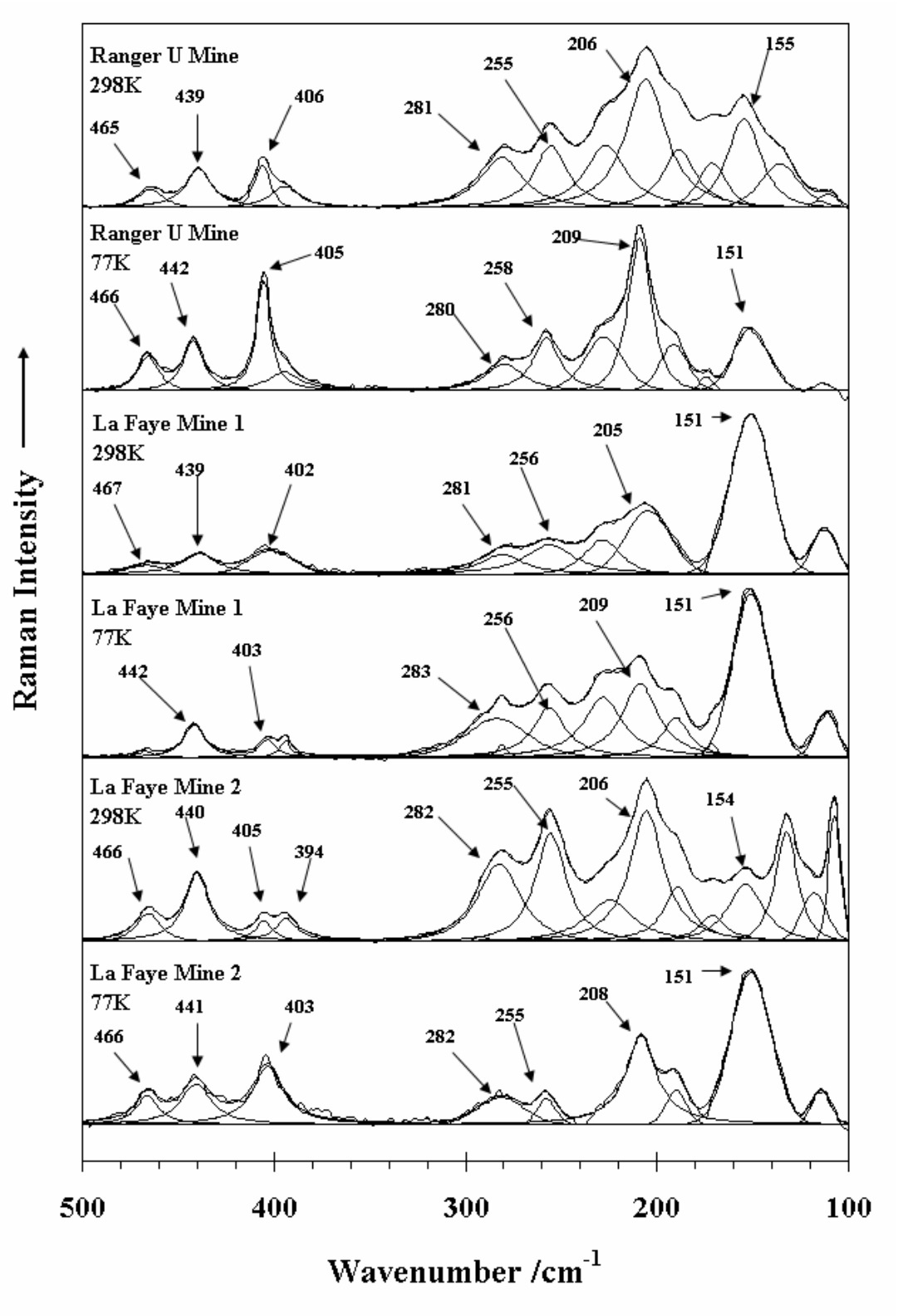
Ranger U Mine
298K
465
439
406
281
255
206
155
Ranger U Mine
77K
466
442
405
280
258
209
151
La Faye Mine 1
298K
467
439
402
281
256
205
151
La Faye Mine 1
77K
442
403
283
256
209
151
La Faye Mine 2
298K
466
440
405
394
282
255
206
154
La Faye Mine 2
77K
466
441
403
282
255
208
151
Raman Intensity
500
400
300
200
100
Wavenumber /cm-1

Figure 3

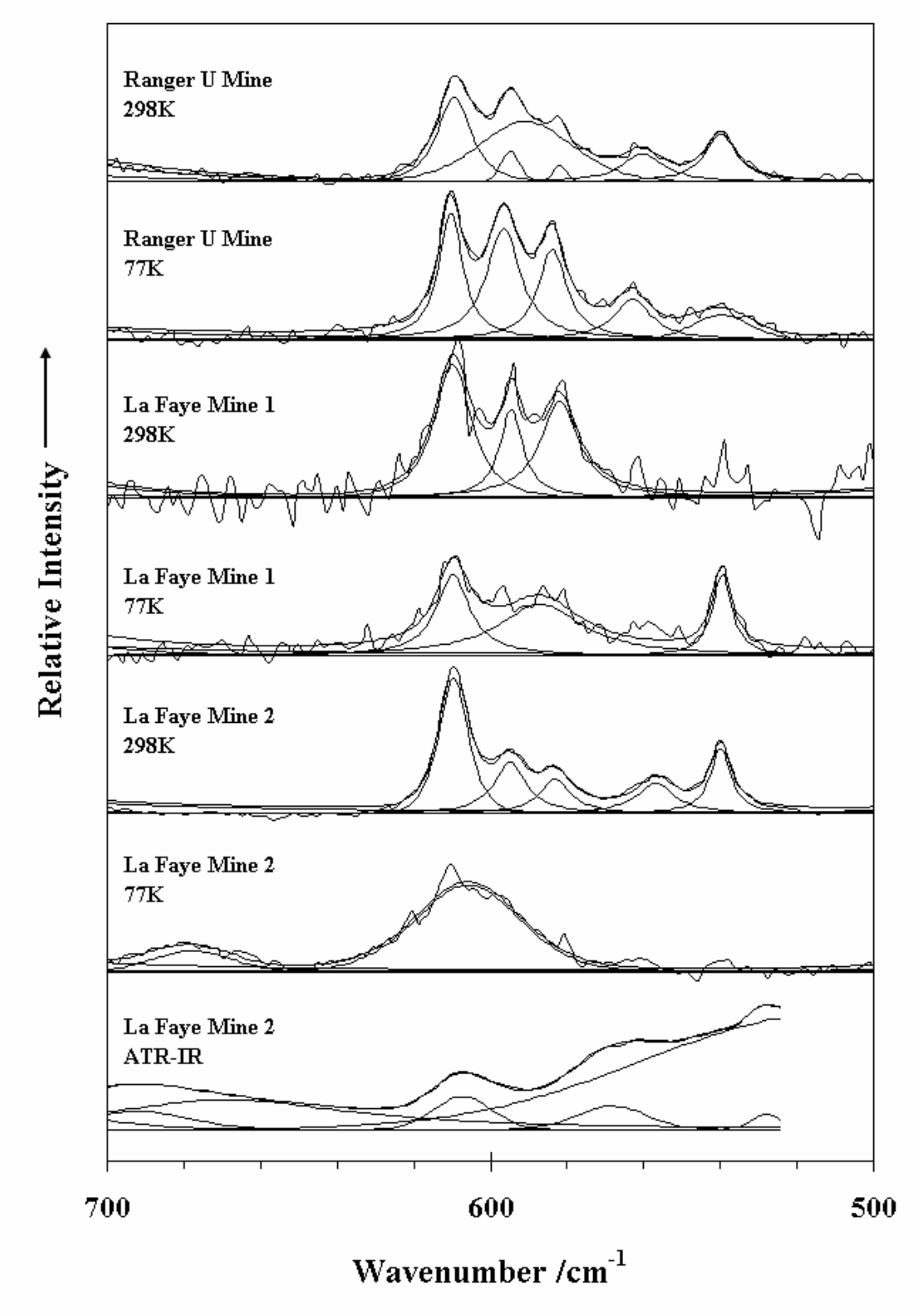
Ranger U Mine
298K
Ranger U Mine
77K
La Faye Mine 1
298K
La Faye Mine 1
77K
La Faye Mine 2
298K
La Faye Mine 2
77K
La Faye Mine 2
ATR-IR
Relative Intensity
700
600
500
Wavenumber /cm-1

Figure 4

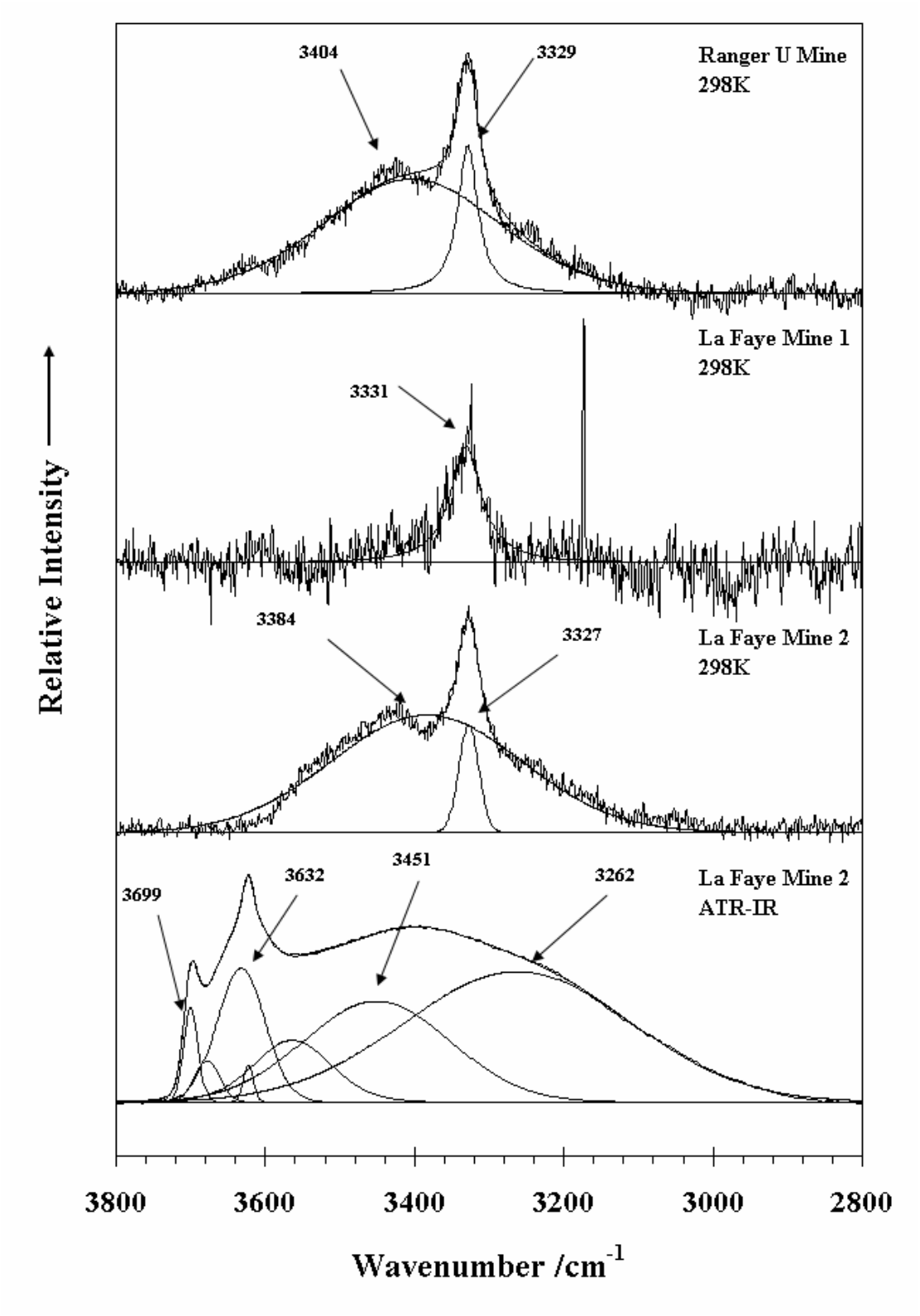
3404
3329
Ranger U Mine
298K
La Faye Mine 1
298K
3331
3384
3327
La Faye Mine 2
298K
3699
3632
3451
3262
La Faye Mine 2
ATR-IR
Relative Intensity
3800
3600
3400
3200
3000
2800
Wavenumber /cm-1

Figure 5